A Multi-UAV Clustering Strategy for Reducing Insecure Communication Range

Jiehong Wu[a], Liangkai Zou[a], Liang Zhao[a,*], Ahmed Al-Dubai[b], Lewis Mackenzie[c], Geyong Min[d]

[a]*Shenyang Aerospace University, Daoyinandajie, Shenyang, China*
[b]*Edinburgh Napier University, Colinton Road, Edinburgh, UK*
[c]*University of Glasgow, Lilybank Gardens, Glasgow, UK*
[d]*University of Exeter, North Park Road, Exeter, UK*

Abstract

Multi-unmanned aerial vehicle (UAV) flight formations can be deployed to monitor large areas. Individual UAVs communicate and exchange information while formation flying. but, such communication presents a security risk. The area between the UAV group range and the group communication range is called the insecurity range and in this region multi-UAV communication can cause serious information leakage. To resolve this problem, this paper considers two aspects, namely, cooperative control and secure communication. To implement cooperative control, a clustering algorithm is presented to accelerate the speed at which the multi-UAV formation converges. By setting the flight control factor to accelerate the convergence of multi-UAV, the UAV group forms a flock. To facilitate secure communication, the hierarchical virtual communication ring (HVCR) strategy is deployed to reduce the boundary of group communication and minimize the insecure range. The effectiveness of the clustering algorithm and HVCR strategy is demonstrated via theoretical analysis and experiments. In the case of 50 and 100 nodes, the results show that the clustering algorithm can facilitate multi-UAV group flocks. In the case of 25, 30, 35 and 40 nodes, the HVCR strategy can reduce the relative size of the insecure range to 65.33%, 62.95%, 61.50% and 60.55%, respectively.

Keywords: Unmanned Aerial Vehicle (UAV), Multi-UAV, Group Communication, Cooperative control, Secure communication.

---

*Corresponding author
    Email addresses: `wujiehong@sau.edu.cn` (Jiehong Wu), `15804065663@163.com` (Liangkai Zou), `lzhao@sau.edu.cn` (Liang Zhao), `a.al-dubai@napier.ac.uk` (Ahmed Al-Dubai), `Lewis.Mackenzie@glasgow.ac.uk` (Lewis Mackenzie), `g.min@exeter.ac.uk` (Geyong Min)

1. Introduction

Recently, unmanned aerial vehicles (UAVs) have been used in various fields including military, civilian, rescue and urban management applications [1–9]. In battlefield operations, UAVs are used to perform various searches and surveillance tasks [10], and the danger of pilot casualties is removed since UAVs do not require human operators in the field. In agriculture, UAVs equipped with hardware devices, such as high-definition digital cameras, spectrum analyzers and thermal infrared sensors, is able to fly over farmland to accurately measure the planted area. The data collected by such UAVs can be used to assess crop risk scenarios, premium rates, and monitor damaged farmland losses. UAVs can quickly implement rescue operations during disasters and communication interruptions due to their minor and flexible operations [11–15].

Currently, multi-UAV are widely deployed to explore locations that are difficult to reach and can quickly deliver goods over complex terrain [16]. During floods, earthquakes and other disasters, multi-UAV can investigate potential route hazards without being affected by road conditions. Compared with a single UAV, multi-UAV can work together cooperatively to accomplish tasks effectively and mitigate the risk of terminating the task due to the damage of a single UAV. A system is required to manage multi-UAV, and the system design should be considered from two aspects, namely, multi-UAV cooperative control and multi-UAV secure communication. Studies of multi-UAV cooperative control have found that multi-UAV systems and biological clusters have notable similarities [17–19]. Biological cluster behavior is a common natural phenomenon observed in different animals, e.g., birds. In a biological cluster, individuals use simple rules and local interactions to produce robust self-organized behavior with high self-adaptability and suitable expendability, akin to intelligent systems. This paper considers the multi-UAV system as a cluster. Each UAV is an individual that follows the Reynolds rules [20] because it tries to stay close to nearby flock-mates, avoid collisions with these flock-mates and match their velocity.

In multi-UAV communication, we assume that UAVs cannot always be connected to a ground base station because the distance between the station and the UAVs will sometimes be too large to allow communication. Thus, a self-organizing network among multi-UAV must be established. A flying ad hoc network (FANET)[21], which is a special form of ad hoc network without a central controller, is suitable for establishing a UAV network. The topology of this network changes quickly and has strong self-organization and self-healing abilities, so that the failure of a node will not affect the network performance. However, security is an issue, because the information in the network is transmitted tirelessly and this is vulnerable to eavesdropping. The conventional security strategy normally applies the existing cryptography mechanisms to ensure the safety of transmission in the higher layers. However, it is still difficult to guarantee the safety of the transmitted messages or the UAV nodes. For example, the transmitted message could be decrypted once the message is captured by the neighboring attackers; UAVs could be attacked by the hidden terminals

(UAV attacker) in the transmission range. This could cause even severe problems in the multi-UAV networks. When the control messages transmitted inside the UAV group, the messages could be captured by the fraud UAVs inside of the coverage of the group members. Therefore, due to the large insecure range during multi-UAV flight, information leakage can take place. To address this problem, a new framework of multi-UAV flight is proposed in which the cooperative control strategy can direct multiple UAVs to the desired location in order to meet communication needs. This paper also presents a clustering algorithm for multi-UAV cooperative control. A new hierarchical virtual communication ring (HVCR) strategy is then proposed for controlling the multi-UAV communication range. Controlling the communication range of UAVs can increase the safety of UAV groups and achieve the goal of safe cooperative flight within the UAV group. The main contributions of this paper are threefold as follows.

1) This paper is the first study that presents the combination of cooperative control and secure communication, which guarantees the secure communication in the scenario of multi-UAV cooperative control flight. Prior studies, e.g., [22], redefined the potential function for cooperative control of multi-UAV but did not address the speed of clustering and secure communication. In [23], the group information exposure problem is presented, and a solution is proposed but cooperative control and UAV group survival time are not considered.

2) The clustering algorithm is implemented in three-dimensional space, which improves the flocking algorithm proposed by Olfati-Saber [24]. During the flocking process, multi-UAV can achieve flocking from a disordered state. If the distance between two nodes is less than a certain threshold, a communication link will be generated between them. By using the flocking algorithm, the distance between all UAVs is approximately equal for communicating with each other to achieve flocking. However, in the flocking algorithm, the initial distance between some UAVs and the UAV group may be large, and the convergence process will be slow. In this paper, to improve the effectiveness of flocking, a clustering algorithm is proposed for these UAVs. The algorithm can identify the UAVs that have no communication links with the UAV group, and the flight control factor is introduced to change the flight speed of these so that the UAV group can converge quickly.

3) After performing the clustering algorithm, an insecure range is observed in the UAV group. Thus, our contribution here is to redefine the speed of the agents, which can make them converge faster so that more communication links can be formed in a shorter time. However, this will result in the boundary UAVs being unable to communicate with the UAV group. Therefore, the movement algorithm is designed to move the boundary UAVs so that the UAV group can communicate effectively. In particular, this movement algorithm could make the UAV nodes move to specified location quickly.

In this paper, FANETs are used as multi-UAV networks. It is assumed that the carrier is a quackster UAV, which is a six-degree-of-freedom vertical UAV that can adjust the flight angle at any time whilst flying. We focus on exploring the communication range. The rest of this paper is organized as follows. Section 2 presents the most relevant works and also shows the motivation of our work.

3

In Section 3, the clustering algorithm is described. In Section 4, the HVCR strategy is presented. In Section 5, a simulation experiment is conducted and the results analyzed. Finally, in the last section, the summary and prospects of the work are presented.

2. Related Work

2.1. Multi-UAV Cooperative Control

A control logic design based on a finite state automaton mode is presented by Meng *et al.* [25]. Addressing the problem of autonomous cooperative takeoff for miniature fixed-wing UAVs, the design integrates four modes of operation: takeoff mode; fly-to-area of operation mode; search mode; and tracking mode. A finite-state automaton (FSA) model of UAV operation is developed to guide UAVs to form clusters based on their current state. Although this method studies the cooperative control of fixed-wing UAVs during takeoff, it does not address quackster devices.

The cooperative control of UAVs is divided into two categories: centralized control and decentralized control. Centralized control schemes use a single controller that requires high computational power; however, dependence on a single unit means that such schemes are not robust. In decentralized control schemes, on the other hand, UAVs each have their own controller; a downside here is that the critical points are difficult to predict and manage when considering collision avoidance. Based on the above two schemes, a bounded cooperative controller method is proposed by Do *et al.* [26]. Here, a p-times differential bump function is introduced to design controllers that yield global asymptotic convergence of a group of mobile agents to a desired formation. Although the method addresses bounded cooperative controllers of multi-UAV, it does not address the problem of multi-UAV communication.

An approach based on the geometric azimuth angle and relative inclination angle is presented by Qu *et al.* [27] to solve the multi-UAV cooperative positioning problem in the presence of GPS transient failures. To obtain the position of a faulty UAV when building the model, this approach necessitates at least two sets of UAV azimuth and inclination angles to achieve the cooperative positioning of the malfunctioning vehicle. Although this approach solves the fault tolerance problem of cooperative positioning, it does not discuss cooperative controlled flight.

While operating in a completely unknown area, multi-UAV can be effectively controlled to maximize search coverage via a communication strategy based on information fusion as presented by Fu *et al.* [28]. The multi-UAV group is stratified, and the first level is selected as the leader. The levels are extended to enable effective communication between the UAVs. The UAVs can then exchange search probability maps with each other through airborne communication equipment, fusing the maps to maximize the search coverage when one UAV overlaps anothers communication range. However, this strategy does not consider secure communication.

4

The flocking algorithm is proposed by Olfati-Saber, enabling multi-UAV to fly cooperatively and reach a relatively stable position. In the flocking process, communication links are produced suitable for the cooperative control of multi-UAV.
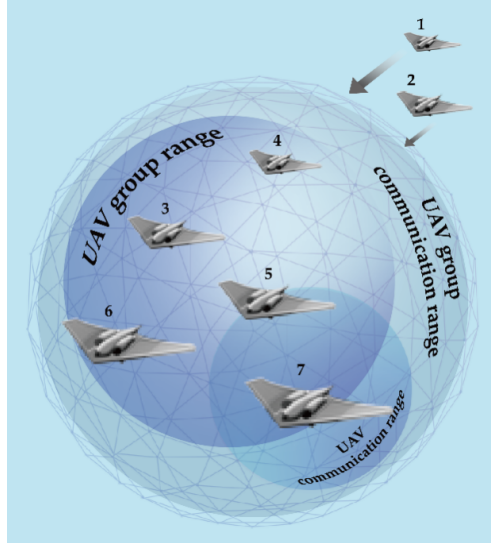

Fig. 1. UAV flocking and communication.

2.2. Multi-UAV Secure Communication

For spatially secure group communication, the problem of weak signal strength between UAVs can be addressed by increasing that strength; however, increasing the signal-to-noise ratio (SNR) can lead to group information exposure. A new method of multi-UAV control with spatially secure communication is presented by Kim et al. In the UAV group, the transmission power gradually decreases from the central nodes to the boundary nodes so that the UAV communication range is variable, thereby securing communication. Despite the fact that this method provides a solution to the UAV group secure communication problem, the power of each UAV must be controlled in a distributed manner. Moreover, because of the different power profiles of the UAVs, individual survival time varies, which leads to the rapid power-depletion death of some group members.

Compared with terrestrial base stations, the advantage of UAV-based stations is their ability to provide on-the-fly communications. The high altitude of UAVs enables them to establish line-of-sight (LoS) communication links, thereby mitigating signal blockages and shadowing. Based on this concept, an algorithm is proposed by Mozaffari et al. to optimize UAV 3D placement and mobility, device-UAV associations, and uplink power control [29]. By constraining device-specific signal-to-interference-plus-noise ratios (SINR), UAV locations, UAV-device associations and optimal uplink transmission power of devices can be determined. Although ideal transmission power is achieved by adjusting

5

the position of the UAV, cooperative control during multi-UAV flight was not discussed in the study.

2.3. Motivations

Above, a survey of current state-of-art multi-UAV cooperative control and secure communication strategies indicates that none of the existing studies of cooperative control and secure communication consider the latter while cooperatively controlling multi-UAV flight. In the cluster, communication must be maintained among UAVs, and tasks must be performed efficiently. In Fig. 1, UAV_3, UAV_4, UAV_5, UAV_6, and UAV_7 can quickly form a cluster, whereas UAV_1 and UAV_2 are too far away to be included. Cooperative control is used to make UAV_1 and UAV_2 fly faster toward the group to form a larger cluster. In the new cluster, communication must be maintained among the UAVs. For example, during the flight of a UAV group, the location of each UAV is not known in advance during group aggregation. Therefore, each UAV communicates with others, each UAV is required to carry signal transmitter. In this way, after the group is formed, all the signal transmitters carried by the UAV will send out signals, and the range of signal coverage of each UAV is the communication range of the UAV mentioned in this paper and the communication range of all the UAV. For the UAV group communication range, this range is different from the scope of the UAV group, which is the union of the range of the UAV group and the communication range of the outer UAV. As shown in Fig. 1, the inner circular area where UAV_3, UAV_4, UAV_5, UAV_6 and UAV_7 are located is defined as the group communication range of this UAV group. In addition, the secure communication refers to reducing the insecure range of the UAV group. We assume that the UAV group range is the detection range which is the area that the UAV group can monitor. In the multi-UAV missions, a detection blind area is not in the detection range of a UAV group if the communication radius is greater than the detection radius of the UAV group. In other words, the detection blind area is the area where UAV group communication range can cover but UAV group cannot monitor. Information leakage occurs when an intruder can obtain the communication message without being detected by the UAV group in the blind area. In this paper, the range of information leakage is defined as the insecure range.

3. Cooperative Control Strategy

In this paper, the UAV dynamic model is used to discretion UAV trajectories and the position of each UAV, velocity and other information. We use the graph theory to describe the topological structure of multi-UAV groups in flight and obtain information about each individual. The clustering algorithm improves flocking to control the UAVs cooperatively. The flocking algorithm itself is derived from the flight behavior of birds in nature where a dynamic hierarchical network is formed. A currently high-level individual plays a leading role, called a leader, and low-level individual behaviors are determined with respect

6

to this leader [30]. In the flocking strategy, the terms α-agent and γ-agent are introduced to describe the relationship among individuals, where the α-agent represents a low-level individual and the γ-agent represents a high-level individual. The γ-agent is the leader of the group and can be considered a gathering point while moving.

The commonly used notations in this paper are listed in Table 1.

Table 1

Notations.

Notations	Description
q_i	Euclidean position of UAV i.
p_i	velocity of UAV i.
u_i	acceleration of UAV i.
w_i	position summarized of UAV i in three dimensions.
N_i	set of neighbor UAVs that UAV i can communicate with i in V.
v_i	velocity of UAV i.
f_i^g	gradient-based term of UAV i.
f_i^d	damping force of UAV i.
f_i^γ	navigational feedback caused by a group. objective of UAV i.
f_i^c	flight control factor of UAV i.
d_i	radius of the agent ball of UAV i.
S_o	the area of the outer circle.
S_1	the area of the inner circle.
A	adjacent matrix.
ε	set of communication links.
R_u	range of UAV group or detection range of UAV group.
R_c	communication range of UAV group.
V	set of UAVs.
k	the number of boundary UAVs.
x	the distance the edge node moves.

3.1. Dynamic Model

In the clustering algorithm, the dynamic model is defined as $q_i^{''} = p_i^{'} = u_i$, where q_i, p_i and $u_i \in R^m (m = 2, 3)$ represent the UAVs location, velocity and acceleration, respectively. The three-dimensional dynamic model is defined as follows:

$$\begin{cases} x^{'} = v_{x'} \\ y^{'} = v_{y'} \\ z^{'} = v_{z'} \end{cases} \tag{1}$$

where $u = [x, y, z]^T \in R^2$ is a state variable, and v_x, v_y, v_z represent the velocity in dimension x, y, z directions, respectively.

The Runge-Kutta [31] method is used to discretize the model (1). The sampling period is set as τ, and w is described as follows:

$$w_{i+1} = w_i + \alpha_1 k_1 + \alpha_2 k_2 + \cdots \alpha_n k_n \tag{2}$$

where

7

$$\begin{cases} k_1 = f(t_i, w_i) \\ k_j = f(t_i + c_j\tau, w_i + \sum_{p=1}^{j-1} a_{jp}k_p) \end{cases} \quad (3)$$

In equation (3), c_j, a_{jp}, α_j are coefficients, where $\alpha_j = \tau c_j$. The Runge-Kutta method is an n-order model, and in our method, $n = 2$. The second-order Runge-Kutta method is as follows:

$$w_{i+1} = w_i + \tau(c_1 k_1 + c_2 k_2) \quad (4)$$

where

$$\begin{cases} k_1 = f(t_i, w_i) \\ k_2 = f(t_i + \tau\lambda_2, w_i + \tau\mu_{21}k_1) \end{cases} \quad (5)$$

3.2. Topological Structure of a UAV

To better explain the effects of distance on communication among UAVs, an undirected graph is used to describe the communication relationship. A graph G is a pair (V, ε) that consists of a set of vertices and edges, where the vertices represent the UAVs and the edges represent the communication links [32]. The adjacency matrix of graph G is expressed as $A = [a_{ij}]$, where $a_{ij} \neq 0 \Leftrightarrow (i, j) \in \varepsilon$. The adjacency matrix is a symmetric matrix $(A = A^T)$. If node i can communicate with node j, then $a_{ij} \neq 0$; otherwise, $a_{ij} = 0$. The neighbors of UAV i are defined as follows:

$$N_i = \{j \in V : a_{ij} \neq 0\} = \{j \in V : (i, j) \in \varepsilon\} \quad (6)$$

The communication radius of a UAV is r $(r > 0)$, and the adjacency set of UAV i is defined as follows:

$$N_i = \{j \in V : \|q_j - q_i\| < r\} \quad (7)$$

The topology structure map of UAV i is shown in Fig. 2. It shows that the communication distances among the UAVs are equal and all UAVs within the communication range of UAV i can communicate with UAV j. The topology of the wireless sensor network with a communication radius is an adjacency network [33].

3.3. Clustering Algorithm Based On the Flight Control Factor

In free space, the flocking algorithm describes the behavior of low-level individuals affected by high-level individuals, and each individual represents a bird in the flock. In the algorithm, an agent is used to describe the individuals. The flocking algorithm can make the agents converge to flocking from a disordered state and ensures that collisions do not occur between agents. The flocking algorithm is described as follows:
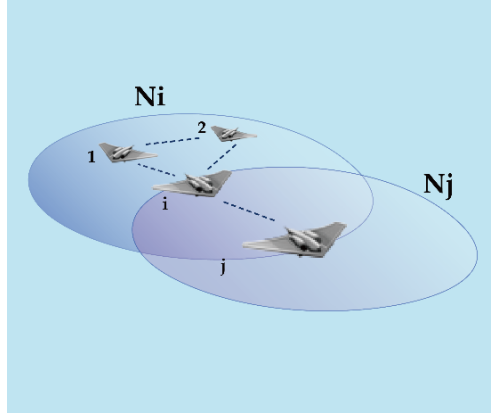
$$u_i = f_i^g + f_i^d + f_i^\gamma \quad (8)$$

8

Fig. 2. UAV communication topology.

where $f_i^g = -\nabla_{q_i} V(q)$ is a gradient-based term, f_i^d is a velocity consensus term that acts as a damping force, and f_i^γ is navigational feedback caused by a group objective.

In the flocking algorithm, there are two virtual forces acting between adjacent agents: attraction and repulsion. Attraction is greater than repulsion when the distance between the two agents exceeds a certain value and, in this situation the two agents will congregate. In the flocking algorithm, all the agents can move gradually, although certain pairs do not have a communication link. From this point, our contribution is that redefines the speed of the agents which can make them converge faster so that more communication links can be formed in a shorter time. Accordingly, the clustering algorithm is proposed, and the flocking algorithm is expressed via a segmented function. The flight control factor is introduced to make the multi-UAV group converge quickly. In the clustering algorithm, an agent is expressed as a UAV. The algorithm is described as follows:

$$\begin{cases} u_i = f_i^d + f_i^\gamma + f_i^c, & \|q_j - q_i\| > d_1 \\ u_i = f_i^g + f_i^d + f_i^\gamma, & \|q_j - q_i\| < d_2 \\ u_i = f_i^\gamma, & otherwise \end{cases} \tag{9}$$

where f_i^c is the flight control factor, defined as,

$$f_i^c = \sum_{j \in N_i} \frac{\kappa}{\|q_j - q_i\|} \tag{10}$$

In (9), $d_1 > d_2, d_1, d_2, \kappa$ are constants. By introducing the flight control factor, the repulsive potential in the flocking algorithm is redefined. In the clustering algorithm, the repulsion value is inversely proportional to the distance between UAVs. The repulsion is smaller when the distance is large so that UAVs converge faster. If the distance between one UAV and others is larger than d_1 during flocking, then the flight control factor will act on the UAV to make it converge quickly. Here, d_1 is much larger than the communication radius of

9

the UAV; therefore, the collision problem during UAV flight does not need to be considered. If the distance is between d_1 and d_2, then navigation feedback will act on the UAV to move it to the virtual leader. If the distance is less than d_2, then the UAV's speed will decrease and the flocking algorithm will be implemented so that all the UAVs reach the flocking state without a collision.

4. Secure Communication Strategy

The HVCR is presented in this paper to address the communication strategy. First, the UAV group is stratified to find the boundary UAVs. Then, the insecure range decreases by reducing the communication radius of these. Finally, the movement algorithm is used to move the boundary UAVs to communicate with the UAV group.

4.1. Hierarchical Virtual Communication Ring

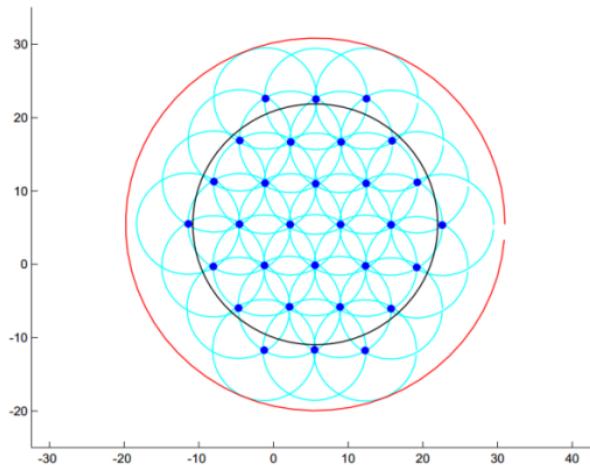#### 4.1.1. Definitions and Group Hierarchical Algorithm

Fig. 3. UAV group communication.

In the paper, to better describe the insecure range, a topology structure of multi-UAV is used to illustrate this range. As shown in Fig. 3, this is a two-dimensional coordinate system, where the X and Y axes represent the latitude and longitude, respectively. So a pair of coordinates (x, y) determines the location of the UAV. The outer circle represents the communication range of the UAV group, and the inner circle represents the range of the UAV group. We assume that the range of the UAV group is the detection range of the UAV group. The annulus between the outer circle and the inner circle is the insecure range, which is defined as follows:

$$S = S_o - S_i \tag{11}$$

10

where S_o is the area of the outer circle and S_i is the area of the inner circle.

In the HVCR strategy, the range and communication range of the UAV group are defined so that the strategy is easier to describe. The two ranges are assumed to be circular regions that can be described by the center and radius. The center of these two ranges is the same, which is described as follows:

$$c = \frac{1}{2}(p_i + p_j), max_{i,j \in N}D(p_i, p_j) \tag{12}$$

where $D(p_i, p_j)$ is the distance between two UAVs, which is described as follows:

$$D(p_i, p_j) = \sqrt{(x_{pj} - x_{pi})^2 + (y_{pj} - y_{pi})^2} \tag{13}$$

where x and y are the coordinates of p.

The radius of the range of the UAV group is described as follows:

$$R_u = \frac{1}{k} \sum_{i=1}^{k} D(p_i - c) \tag{14}$$

where p represents the location of the UAV and k is the number of boundary UAVs. The radius of the UAV group communication range can be obtained using the radius of the UAV group range, which is described as follows:

$$R_c = R_u + r \tag{15}$$

where r is the radius of the boundary UAVs communication range, which can be obtained via theoretical analyses and experimentation..

Algorithm 1 Group hierarchical algorithm.

Input: $P_{1...N}$, a_{ij}
Output: edge_nodes

1: Queue level _node
2: The number of level _node $j = 2$
3: $k = 0$;
4: Push c to level_node
5: level_node(1)=c
6: The number points of level_node(j) $i = 1$
7: **while** !isEmpty(level_node) **do**
8:     **if** $i == 0$ **then**
9:         $j = j + 1$
10:        $i = k$
11:    **end if**
12:    Pop L from level_node($j - 1$)
13:    $i = i - 1$
14:    **while** there are neighbor nodes of L **do**
15:        Find neighbor nodes NN of L using a_{ij}
16:        level_node(j)=level_node(j)+NN
17:        $k = k + 1$;
18:    **end while**
19: **end while**
20: level_node(j);

Algorithm 1 layers UAV group nodes and finds the outermost node. The final output of the algorithm is the set of outer nodes. We use the queue as the intermediate storage structure. Firstly, the central node is set as a node in the first-layer and enters the queue. When searching for the second-layer node, the first-layer node is queued, and the adjacent nodes of the first-layer node are scanned. If the adjacent node is not scanned, it will be queued. If a first-layer node scans as the center node, this first-layer node is also a second-layer node. The scanning expends in the above way until all nodes have been scanned. Therefore, the basic operation of the algorithm is to queue the nodes that are not scanned. If the number of nodes is N, the time complexity of the algorithm is $O(N)$. In the algorithm, the queue is used as the intermediate structure for the data storage and the space occupancy is at most N. Therefore, the space complexity of the algorithm is $O(N)$.

4.1.2. Optimal Communication Radius

The radius of the boundary node has a critical value when the radius of the boundary UAV gradually decreases. In this case, the insecure range of the UAV group is the smallest. We define the critical value as the optimal communication radius of the boundary UAV.
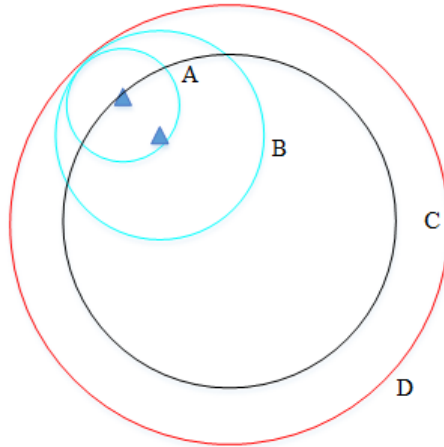

Fig. 4. Examplary diagram of communication.

As shown in Fig. 4, circles A and B are the communication range of the outer UAV and inner UAV respectively. Circle C is the UAV group range, which is also the detection range. Circle D is the UAV group communication range. In this paper, the optimal communication radius of the outer UAV is found via the theoretical proof and experimental verification. The theoretical proof is given below and the experimental analysis is given in Section 4.2. The outer UAVs can communicate with the inner UAVs effectively. In addition, the insecure range is minimal. The optimal communication radius is defined as follows:

$$r \in \{0 < r < r_B : C_A \cap C_B = C_A, d_r = r_B - r_A, A \in N_o, B \in N_i\} \qquad (16)$$

where C_A represents the communication range of the outer UAVs shown in circle A; C_B represents the communication range of the inner UAVs shown in circle B, which intersects with C_A; d_r is the distance between two circle centers; R_B is the radius of circle B; R_A is the radius of circle A; N_o represents the collection of the outer UAVs, and N_i represents the collection of the inner UAVs.

The optimal communication radius is determined as follows. To ensure that circle D is the group communication range, circle D must be tangent to either circle A or circle B. In the process of reducing the range of circle A, circle A and circle B will be inscribed. Before reaching this case, circle D should be tangent to circle A. If the range of circle$A$ continues to decrease, then circle D will be tangent to circle B. However, the range of circle B is not changed because node B is the inner UAV; thus, the range of the circle D is not changed.

Therefore, the critical case is reached when circles A, B, and D are all tangent. At this point, even if the range of circle A continues to decrease, circle D will be unchanged and remain tangent to circle B. In the critical case, the radius of circle A is the optimal communication radius. After the experiment, by continuously reducing the communication range of the boundary nodes, the insecure area is calculated. It is found that when the insecure area reaches a minimum, the optimal communication radius of the boundary node is obtained. The optimal radius of circle A was found to be half of circle B.

4.2. Movement Algorithm

After reducing the communication range of the boundary UAVs, the range is not enough to reach their neighbours while they are at the extremity of the cluster. Therefore, the movement algorithm is designed to circulate the boundary UAVs towards the group center so that they can communicate with the UAV group.
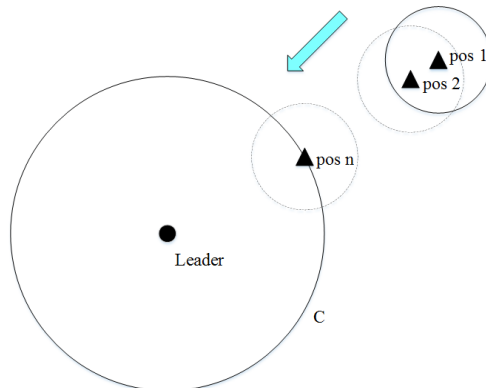

Fig. 5. Movement algorithm.

Fig. 5 shows an example to present the idea of movement algorithm. In this figure, the Leader is the location of the virtual leader, while C represents the scope of the unmanned unit, and the edge node is in the pos 1. When the edge UAV node reduces the communication range, the edge UAV cannot communicate with the inner node of the group. Therefore, it is required to move to the center of the group, and because of the presence of the Leader, the direction of movement can be determined. The final edge node moves to the pos n that is able to communicate with the group.

Algorithm 2 Movement algorithm.

Input: a_{ij}, point_center, $p_{1\ldots N}$,r
Output: the position of edge_point

1: **for** $i = 1$ to N **do**
2:     Find the edge_point using a_{ij}
3: **end for**
4: **for** $j = 1$ to N **do**
5:     **if** j is in the edge_point **then**
6:         **for** $i = 1$ to N **do**
7:             **if** $i! = j$ **then**
8:                 **if** $\mid p_j - p_i \mid < \frac{r}{2}$ **then**
9:                     b =false
10:                    break
11:                **else**
12:                    b =ture
13:                **end if**
14:            **end if**
15:        **end for**
16:        **if** b **then**
17:            $p_j \to point\_center$
18:        **end if**
19:    **end if**
20: **end for**

The movement algorithm mainly finds the nodes in the edge nodes whose distance from the inner node is greater than $r/2$, and then makes these nodes move towards the group center. The nodes that meet the above requirements are a set called M. In this algorithm, the appropriate step size s can be formulated as:

$$s = \frac{R_u}{\jmath} \tag{17}$$

where $\jmath$ is a constant. As shown in Fig. 5, s is the distance between pos 1 and pos 2. Let the nodes in set C slowly approach the group center with step size s. When the distance between a node in set M and any node in the group is less than $r/2$, move the node out of the set. Through the above steps, until there is no node in the set M, then the moving algorithm ends. By introducing the movement algorithm, the nodes in the group can move to the group center in the presence of repulsive force, so that the edge node communicates with the inner node of the group. After the movement algorithm ends, the communication range of all edge nodes is reduced to half, and both can communicate effectively with the inner nodes. Hence, the time complexity of the algorithm is O(n^2).

14

There are no extra spatial variables used in the algorithm. Therefore, the space complexity of the algorithm is O(1).

Algorithm 2 lists the movement algorithm in pseudocode, a_{ij} is the adjacency matrix of the UAVs; p_{center} denotes the center of the UAV group; $p_1...p_N$ are the position information of N UAVs; and r represents the radius of communication range.

5. Experimental Results and Analysis

For the analysis conducted in this study, experiments are carried out using MATLAB [34]. The simulation of the clustering strategy shows the movement position of the UAVs in three-dimensional space. The movement speed variation curve of the UAVs is displayed in this section, and the flocking algorithm is compared with the clustering algorithm. The insecure range "change value" and the group communication range change value are given. Besides, some simulation parameters are listed in Table 2. As show in Table 2, now, the maximum flight velocity of the commercial DJI UAV is $20m/s$. In order to reduce the calculation, we assume that the velocity of the UAV is between 0 and $2m/s$. We scattered the UAV over a cube area between $-30km$ and $30km$, which is enough to simulate the random environment.

Table 2

The simulation parameters.

The size of UAV group	25 nodes, 30 nodes, 35 nodes, 40 nodes
Distance segmentation coefficient $\jmath$	30
The velocity of UAV	Random numbers between 0 and 2 m/s
The coordinates of UAV	Random numbers between -30 and 30 km
Adjacency matrix a_{ij}	All zero matrices
Simulation duration	300 seconds

In the experiment, N points are generated randomly to conform to the normal distribution. The specific parameters are set as in the Runge-Kutta method: $\lambda_2 = \mu_{21} = 0.5$, $c_1 = 0$, and $c_2 = 1$. The initial adjacency matrix a_{ij} is a zero matrix. In the clustering algorithm, $\kappa = 0.3$, $d_1 = 21$, and $d_2 = r = 8.4$.

5.1. Clustering Algorithm Simulation Experiment

5.1.1. Clustering Effect Analysis

As in Fig. 6, this is a three-dimensional coordinate system. The X,Y and Z axes represent the longitude, latitude and altitude of the UAV, respectively. We tested fifty points and a hundred points. In the iterative process of the UAV group, a higher degree of convergence represents more communication links. The smoothness of group convergence can be reflected by the change curve of the communication link with the number of iterations. The result is that a smoother curve denotes more efficient convergence.

The clustering algorithm can make the UAVs converge from a disordered state to flocking and ensure that no collisions occur between the UAVs. After

15

(a) Fifty-point clustering effect comparison

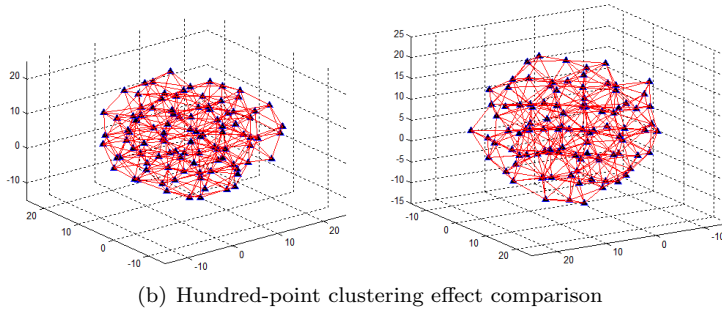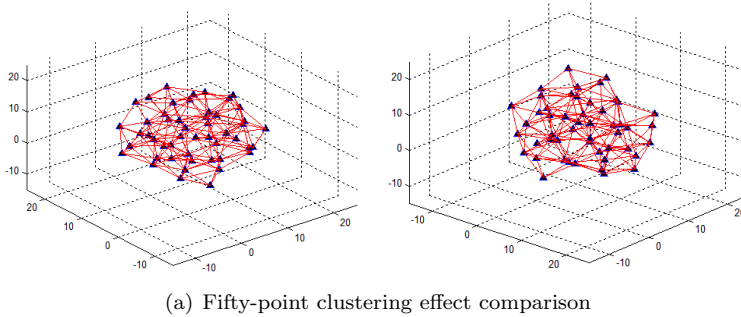(b) Hundred-point clustering effect comparison

Fig. 6. Comparison of the experimental results.

the execution of the algorithm, the communication links between adjacent UAVs are generated and evenly distributed in space.

5.1.2. UAV Flight State Analysis

In the clustering process of the UAV group, all the UAVs experience conver-
gence, divergence, reconveyance, and other processes. As show in Fig. 7, the axial direction X represents the number of algorithm iterations, while the axial direction Y represents the number of communication links, respectively. By analyzing the velocity curve, the clustering process can be clearly observed. Initially, all UAVs follows a normal distribution. When the distance between them is greater, the force of attraction is larger and, because force is proportional to acceleration, the acceleration of the UAV is also larger. When the UAV moves to a balanced position, the attraction is equal to the repulsion, acceleration is 0, and the velocity is highest. All UAVs maintain the current movement direction and continue to converge. Then, the attraction drops below the repulsion, the direction of acceleration is opposite to the velocity direction, and so the vehi-
cle decelerates gradually. When the velocity reaches 0, the repulsion reaches a maximum, and the reverse acceleration is largest, so the UAVs begin to diverge. By cycling through this process, all UAVs finally reach the flocking state.

The comparison between the clustering algorithm and the flocking algorithm
at 50 vehicles in Fig. 8 shows that the clustering algorithm leads to rapid

16
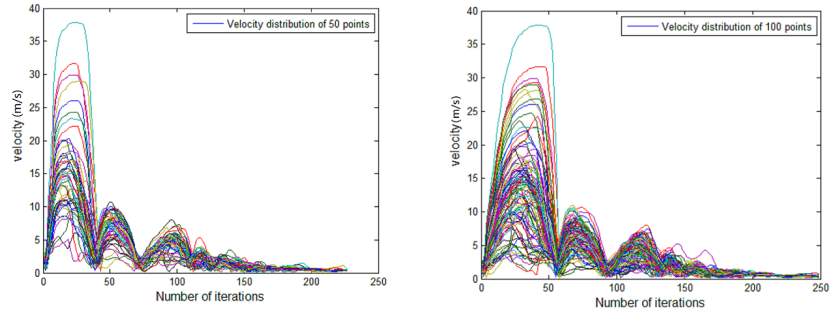
(a) Velocity distribution of Fifty UAVs (b) Velocity distribution of hundred UAVs
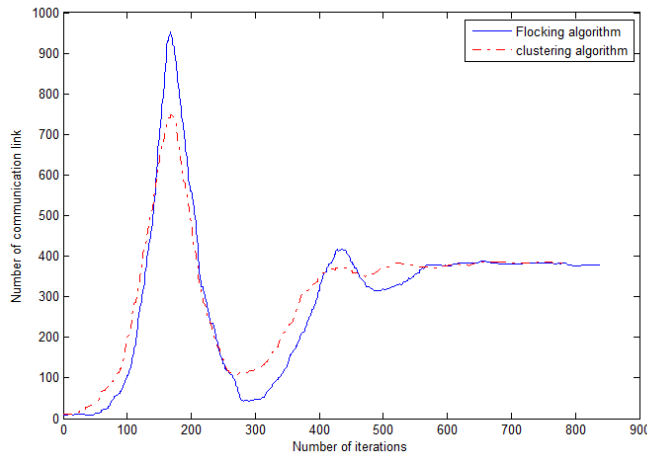
Fig. 7. Velocity curve in the clustering algorithm.

Fig. 8. Comparison of communication link changes.

initial convergence of the UAVs and generates more communication links than the flocking algorithm. As the number of iterations increases, the clustering algorithm rapidly forms a flocking state, and the flocking process is more stable with fewer iterations.

435   We can analyze Fig. 7 based on multi-UAV velocity changes. When the two curves reach the maximum value for the first time, i.e. the position of the first wave crest, the greatest number of communication links between the UAVs is achieved. Now, the multi-UAV reach the first flocking state and the speed of the UAVs is zero. Thereupon, the UAV group begins to diverge, with the reverse

440   speed becoming larger and the number of communication links beginning to decrease. Arriving at the first wave trough, the divergence process ends and the speed is zero. Then, the UAV group continues to converge. Finally, the number of communication links remains stable and the speed tends toward zero.

17

5.2. Hierarchical Virtual Communication Ring Experiment

In this section, points are used to represent the UAVs. After running the clustering algorithm, all points reach the flocking state. Then, the HVCR strategy is used to rearrange the points. The specific process is as follows:

1) All points are stratified, and the HVCR strategy is applied to the boundary points. All the points are affected by the virtual force in the clustering algorithm.

2) The communication range of edge nodes is reduced. In this way, the edge nodes cannot communicate effectively with the inner nodes, so the edge nodes must move towards the group center. However, due to the repulsion force, the node cannot move to the group center on its own, so the moving algorithm is added to make it act on the repulsion force in the group and move the edge node.

3) The movement algorithm is used to move the boundary points to ensure that these can effectively communicate with the group.

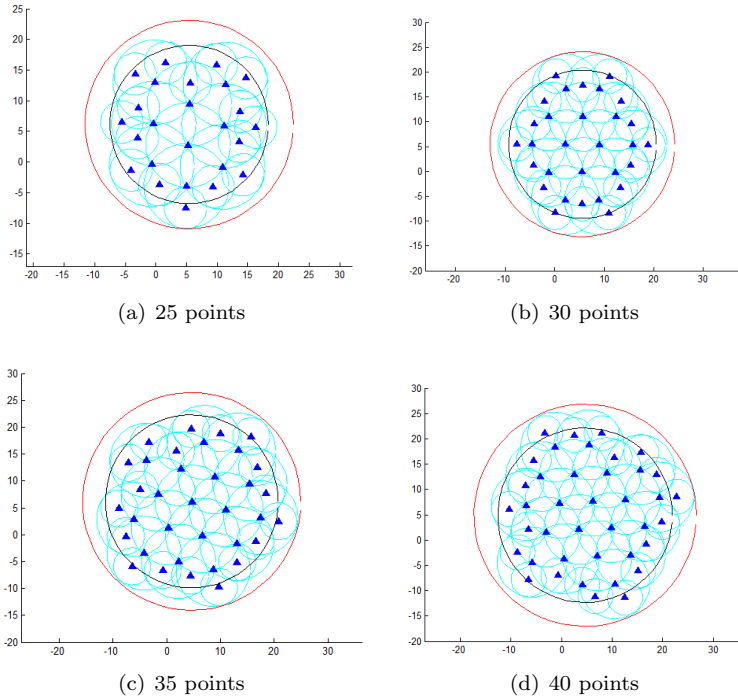(a) 25 points   (b) 30 points

(c) 35 points   (d) 40 points

Fig. 9. Hierarchical virtual communication ring example.

The experimental results at 25, 30, 35 and 40 points are shown in Fig. 9, indicating that in order to improve the security of uav group, all boundary points communicate with the inner point, reducing the unsafe distance. As shown in Fig. 9, although the number of points is different, the HVCR strategy can reduce the communication range of the boundary points and make them

18

communicate with the inner points. The following experimental data show that this strategy can appropriately reduce the insecure range.

5.3. Performance Analysis of the Hierarchical Virtual Communication Ring

5.3.1. Comparison Experiment

In this section, the curves representing the UAV group range and the UAV group communication range after executing this strategy are given. Fig. 10 shows the comparison at 25 points, 30 points, 35 points, and 40 points. This curve shows that the area of communication decreases as the number of iterations increases.
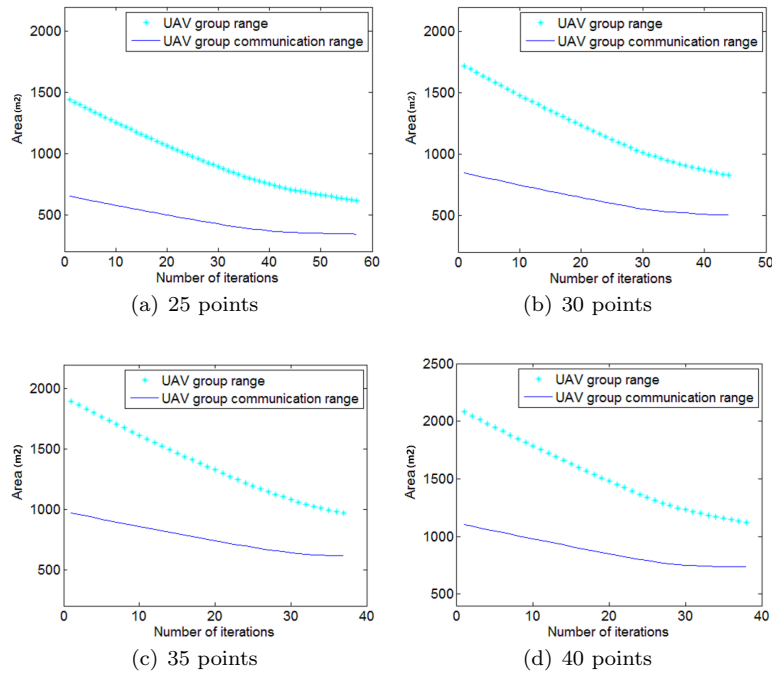

(a) 25 points   (b) 30 points

(c) 35 points   (d) 40 points

Fig. 10. UAV group range and UAV group communication range comparison.

Fig. 10 shows that the HVCR strategy produces a stable effect when different points are set in the experiment. As the number of iterations increases, the communication range of the boundary points decreases. Because of the role of the virtual force, boundary points move closer to the group center so that the group range is reduced, which decreases the group communication range. The UAV group range is approximately equal to the UAV communication range to ensure secure communication of the UAV group.

5.3.2. Experiment Data

Table 3 shows the data of the UAV group range, the UAV group communication range and the insecure range at 30 points. The data for iteration numbers of

19

Table 3

Data on the hierarchical communication ring with 30 points.

Name of range	1	2	$\cdots$	43	44
UAV group range	845.48	834.25	$\cdots$	502.52	501.39
UAV group communication range	1720.95	1693.28	$\cdots$	835.36	825.78
Insecure area range	875.47	859.04	$\cdots$	332.84	324.39

Table 4

Change data of hierarchical communication ring.

Name of proportion	25	30	35	40
Proportion that is reduced in the UAV group range	47.66%	40.70%	36.53%	33.33%
Proportion reduced of the UAV group communication range	54.55%	52.02%	48.73%	46.12%
The proportion reduced of the insecure range	65.33%	62.95%	61.50%	60.50%

1, 2, 43 and 44 are given in the table, rounded to two decimal places. The results in the table show that the UAV group range decreases from 845.48 to 501.39 (40.70%). The UAV group communication range decreases from 1720.95 to 825.78 (52.02%). The insecure range decreases from 875.47 to 324.39 (62.95%). The data from the other cases are not displayed. Table 4 shows the proportions of the reduction in the UAV group range, the UAV group communication range and the insecure range in the case of 25 points, 30 points, 35 points and 40 points.

In the case of 25 points, the UAV group range decreases by 47.66%, the UAV group communication range decreases by 54.55%, and the insecure range decreases by 65.33%. In the case of 35 points, the UAV group range decreases by 36.53%, and the UAV group communication range decreases by 48.73%, and the insecure range decreases by 61.50%. In the case of 40 points, the UAV group range decreases by 33.33%, the UAV group communication range decreases by 46.12%, and the insecure range decreases by 60.55%.

5.3.3. Mathematical Derivation and Analysis of the Proportional Decrease in the Insecure Range

As shown in Table 4, as the number of points increases the proportionate size of the insecure range decreases, which is consistent with the results deduced by the following formulas. The specific mathematical derivation of the proportion reduction of the insecure range is given below.

Initially, the radius of the UAV group range is r_1; the radius of the UAV group communication range is r_2; and the communication radius of the UAV is d. During the process of moving the boundary UAVs, the radius of the UAV group range decreases by x, the communication radius of the boundary UAVs decreases by half, and the radius of the UAV group communication range decreases by $x + d/2$. It is assumed that $r_2 = r_1 + d$. In practice, the UAV

group range is a circle and the boundary UAVs are uniformly distributed in the edge of the circle. The UAV group range does not cover all the boundary UAVs; therefore, the r_2 value in the assumption may have slight deviations, but these do not affect this derivation. The reduction of the UAV group range is as follows:

$$y_1 = \pi r_1^2 - \pi (r_1 - x)^2 \tag{18}$$

The reduction of the UAV group communication range is as follows:

$$y_2 = \pi r_2^2 - \pi [r_2 - (x + \frac{d}{2})]^2 \tag{19}$$

The insecure range is the difference between the UAV group communication range and the UAV group range:

$$y = y_2 - y_1 \tag{20}$$

The equation $r_2 = r_1 + d$ is brought into the equation (19), and the simplified form is as follows:

$$y = \pi [\frac{3}{4} d^2 + d(x + r_1)] \tag{21}$$

Therefore, the proportion of the insecure range reduction is as follows:

$$\sigma = \frac{y}{\pi r_2^2 - \pi r_1^2} = \frac{4r_1 + 4x + 3d}{8r_1 + 4d} \tag{22}$$

In equation (22), the proportion of the insecure range decrease is related to r_1, x and d. In the experiments, when the number of points is set to a lower value, the proportion is greatly affected by x and d. If the number of points is higher, $r_1 >> x$ and $r_1 >> d$, is significantly affected by r_1. When the UAV group range is increased enough, approaches 50%.

Fig. 11, (a), (b), (c), and (d) show the insecure area range change for 25 points, 30 points, 35 points and 40 points respectively. The experimental results show that the HVCR strategy achieves the expected goal which allows multi-UAV to maintain secure communication during cooperative flight.

6. Conclusion

The paper explores communication security in multi-UAV and the cooperative control of multi-UAV during flight. The study has introduced two strategies, namely clustering and HVCR, to accelerate the speed at which multi-UAV formations converge, and to reduce the boundary of group communication, minimizing the insecure range. In the clustering strategy, the Runge-Kuta method is used to discretion the UAVs trajectory and obtain the UAVs location, speed and other information. The cluster algorithm is used for multi-UAV cooperative control, and additional communication links can be generated during flight:

21

(a) 25 points   (b) 30 points

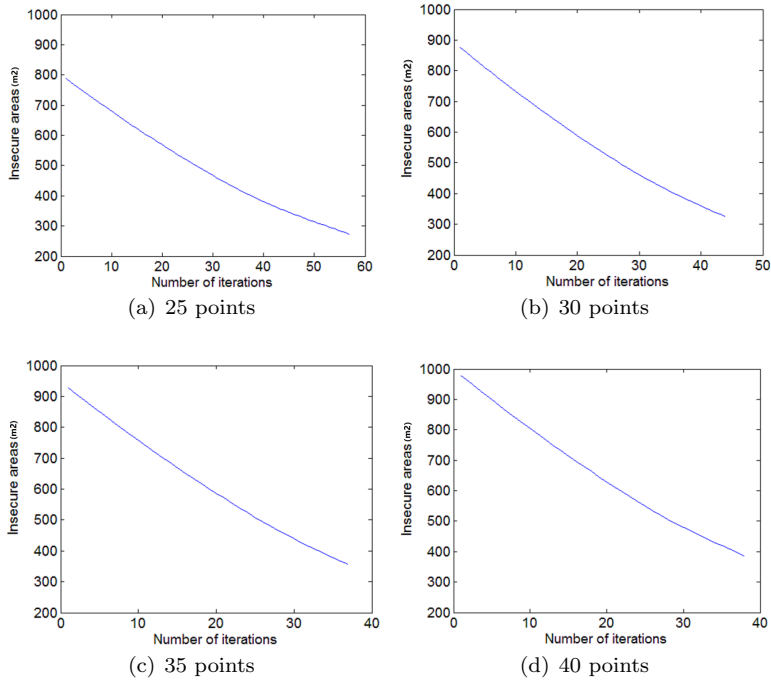(c) 35 points   (d) 40 points

Fig. 11. UAV group insecure communication ranges.

the UAV group achieves a relatively stable state faster and more smoothly, thereby realizing flocking. For communication, the HVCR strategy is proposed and its effectiveness demonstrated. The optimal communication radius of the outer UAVs is obtained, and the movement algorithm is used to position the outer UAVs at the desired location. The results show that the HVCR strategy effectively reduces the insecure range of the UAV group and ensures secure communication of the group.

Our future plan is to analyze the multi-UAV secure communication range problem from the perspective of communication theory. By controlling the intensity, frequency, and wavelength of the signal transmitted by the UAVs, the position of the vehicles can be adjusted so that group members can be cooperatively controlled while communicating with one another. Thus, the secure communication range between UAVs has the potential to be further improved.

ACKNOWLEDGMENT

22

References

[1] L. Gupta, R. Jain, G. Vaszkun, Survey of important issues in UAV communication networks, IEEE Communications Surveys & Tutorials 18 (2) (2016) 1123–1152. `doi:10.1109/COMST.2015.2495297`.

[2] S. Hung, S. Givigi, A q-learning approach to flocking with UAVs in a stochastic environment, IEEE Transactions on Cybernetics 47 (1) (2017) 186–197. `doi:10.1109/TCYB.2015.2509646`.

[3] P. Sun, A. Boukerche, Q. Wu, Theoretical analysis of the target detection rules for the UAV-based wireless sensor networks, 2017, pp. 1–6. `doi: 10.1109/ICC.2017.7997348`.

[4] S. Koulali, E. Sabir, T. Taleb, M. Azizi, A green strategic activity scheduling for UAV networks: A sub-modular game perspective, IEEE Communications Magazine 54 (5) (2016) 58–64. `doi:10.1109/mcom.2016.7470936`.

[5] J. Pei, Development trends of civil UAV industry and its applications in network & communication field, Telecom Engineering Technics & Standardization.

[6] F. Luo, C. Jiang, S. Yu, J. Wang, Y. Li, Y. Ren, Stability of cloud-based UAV systems supporting big data acquisition and processing, IEEE Transactions on Cloud Computing pp (99) (2017) 1–1. `doi:10.1109/TCC.2017.2696529`.

[7] J. Wang, C. Jiang, Z. Han, Y. Ren, L.Hanzo, Taking drones to the next level: Cooperative distributed unmanned-aerial-vehicular networks for small and mini drones, IEEE Vehicular Technology Magazine 12 (3) (2017) 73–82. `doi:10.1109/MVT.2016.2645481`.

[8] F. Tseng, T. T. Liang, C. Lee, L. Chou, H. Chao, A star search algorithm for civil UAV path planning with 3G communication, 2014, pp. 942–945. `doi:10.1109/IIH-MSP.2014.236`.

[9] U. Cekmez, M. Ozsiginan, O. K. Sahingoz, Multi colony ant optimization for UAV path planning with obstacle avoidance, 2016, pp. 47–52. `doi: 10.1109/ICUAS.2016.7502621`.

[10] H. Qiu, H. Qiu, From collective flight in bird flocks to unmanned aerial vehicle autonomous swarm formation, Chinese Journal of Engineering 39 (3) (2017) 317–322. `doi:10.13374/j.issn2095-9389.2017.03.001`.

[11] Y. Sun, J. Zhang, F. Yang, Y. Wang, Z. Wei, Preliminary application of UAV remote sensing system in storm surge disaster loss assessment, Ocean Development & Management.

[12] M. Xiong, D. Zeng, H. Yao, Y. Li, A crowd simulation based UAV control architecture for industrial disaster evacuation, in: IEEE Vehicular Technology Conference, 2016. `doi:10.1109/VTCSpring.2016.7504062`.

[13] M. Erdelj, E. Natalizio, UAV-assisted disaster management: Applications and open issues, 2016, pp. 1–5. `doi:10.1109/ICCNC.2016.7440563`.

[14] J. Sun, B. Li, Y. Jiang, C. Wen, A camera-based target detection and positioning UAV system for search and rescue (SAR) purposes, Sensors 16 (11) (2016) 1178. `doi:10.3390/s16111778`.

[15] M. A. Goodrich, B. S. Morse, D. Gerhardt, J. L. Cooper, M. Quigley, J. A. Adams, et al., Supporting wilderness search and rescue using a camera-equipped mini UAV: Research articles, Journal of Field Robotics 25 (2008) 89–110. `doi:10.1002/rob.20226`.

[16] C. Rasche, C. Stern, L. Kleinjohann, B. Kleinjohann, A distributed multi-UAV path planning approach for 3D environments, 2012, pp. 7–12. `doi:10.1109/ICARA.2011.6144847`.

[17] J. Wang, V. Patel, C. A. Woolsey, N. Hovakimyan, D. Schmale, L1 adaptive control of a UAV for aerobiological sampling, 2007, pp. 4660–4665. `doi:10.1109/ACC.2007.4283121`.

[18] L. Techy, C. A. Woolsey, D. G. Schmale, Path planning for efficient UAV coordination in aerobiological sampling missions, 2008, pp. 2814–2819. `doi:10.1109/CDC.2008.4739456`.

[19] J. Wu, Y. Cao, X. Shi, , C. Yang, Research of cooperative control based on multiple UAVs secure communications, 2016, pp. 135–140. `doi:10.1109/IMCCC.2015.36`.

[20] C. W. Reynolds, Flocks, herds and schools: A distributed behavioral model 21 (4) (1987) 25–34. `doi:10.1145/37401.37406`.

[21] I. Bekmezci, O. K. Sahingoz, . Temel, Flying Ad-Hoc networks (FANETs): A survey, Ad Hoc Networks 11 (3) (2013) 1254–1270. `doi:10.1016/j.adhoc.2012.12.004`.

[22] J. Sun, J. Tang, S. Lao, Collision avoidance for cooperative UAVs with optimized artificial potential field algorithm, IEEE Access PP (99) (2017) 18382–18390. `doi:10.1109/ACCESS.2017.2746752`.

[23] S. W. Kim, S. W. Seo, Cooperative unmanned autonomous vehicle control for spatially secure group communications, IEEE Journal on Selected Areas in Communications 30 (5) (2012) 870–882. `doi:10.1109/JSAC.2012.120604`.

[24] R. Olfati-Saber, Flocking for multi-agent dynamic systems: algorithms and theory, IEEE Transactions on Automatic Control 51 (3) (2006) 401–420. `doi:10.1109/TAC.2005.864190`.

[25] M. Wei, Z. He, R. Su, P. Yadav, R. Teo, L. Xie, Decentralized multi-UAV flight autonomy for moving convoys search and track, IEEE Transactions on Control Systems Technology PP (99) (2016) 1480–1487. `doi:10.1109/ TCST.2016.2601287.`

[26] K. D. Do, Bounded controllers for formation stabilization of mobile agents with limited sensing ranges, IEEE Transactions on Automatic Control 52 (3) (2007) 569–576. `doi:10.1109/TAC.2007.892382.`

[27] Y. Qu, J. Wu, B. Xiao, D. Yuan, A fault-tolerant cooperative positioning approach for multiple UAVs, IEEE Access PP (99) (2017) 1–1. `doi:10. 1109/access.2017.2731425.`

[28] X. Fu, X. Gao, Network building and communication strategy designing for multi-UAVs cooperative search, 2017, pp. 1–5. `doi:10.1109/ICARCV. 2016.7838778.`

[29] M. Mozaffari, W. Saad, M. Bennis, M. Debbah, Mobile unmanned aerial vehicles (UAVs) for energy-efficient internet of things communications, IEEE Transactions on Wireless Communications 16 (11) (2017) 7574–7589. `doi:10.1109/TWC.2017.2751045.`

[30] M. Nagy, Z. Akos, D. Biro, T. Vicsek, Hierarchical group dynamics in pigeon flocks, Nature 464 (7290) (2010) 890–893. `doi:10.1038/ nature08891.`

[31] J. Stoer, R. Bulirsch, Beitrag zur Nherungsweisen Integration totaler Differentialgleichungen, Numerische Mathematik 2, Springer, 2018.

[32] E. Klavins, Communication complexity of multi-Robot systems, Algorithmic Foundations of Robotics V 7 (2004) 275–292. `doi:10.1007/ 978-3-540-45058-0_17.`

[33] I. F. Akyildiz, S. Weilian, Y. Sankarasubramaniam, E. Cayirci, A survey on sensor networks, IEEE Communications Magazine 40 (8) (2002) 102–114. `doi:10.1109/MCOM.2002.1024422.`

[34] P. I. Corke, A robotics toolbox for MATLAB, IEEE Robotics & Automation Magazine 3 (1) (2002) 24–32. `doi:10.1109/100.486658.`